Smart Structures and Systems, *Vol. 16, No. 1 (2015) 141-162*
DOI: http://dx.doi.org/10.12989/sss.2015.16.1.141

Stochastic micro-vibration response characteristics of a sandwich plate with MR visco-elastomer core and mass

Z.G. Ying[1a], Y.Q. Ni[2b] and Y.F. Duan[*3]

[1]*Department of Mechanics, School of Aeronautics and Astronautics, Zhejiang University, Hangzhou 310027, P.R. China*
[2]*Department of Civil and Environmental Engineering, The Hong Kong Polytechnic University, Hung Hom, Kowloon, Hong Kong*
[3]*Department of Civil Engineering, College of Civil Engineering and Architecture, Zhejiang University, Hangzhou 310058, P.R. China*

(Received July 24, 2014, Revised August 31, 2014, Accepted September 3, 2014)

Abstract. The magneto-rheological visco-elastomer (MRVE) is used as a smart core to control the stochastic micro-vibration of a sandwich plate with supported mass. The micro-vibration response of the sandwich plate with MRVE core and supported mass under stochastic support motion excitations is studied and compared to evaluate the vibration suppression capability. The effects of the supported mass and localized magnetic field on the stochastic micro-vibration response of the MRVE sandwich plate are taken into account. The dynamic characteristics of the MRVE core in micro-vibration are described by a non-homogeneous complex modulus dependent on vibration frequency and controllable by applied magnetic fields. The partial differential equations for the coupled transverse and longitudinal motions of the MRVE sandwich plate with supported mass are derived from the dynamic equilibrium, constitutive and geometric relations. The simplified ordinary differential equations are obtained for the transverse vibration of the MRVE sandwich plate under localized magnetic fields. A frequency-domain solution method for the stochastic micro-vibration response of sandwich plates with supported mass is developed based on the Galerkin method and random vibration theory. The expressions of frequency-response functions, response power spectral densities and root-mean-square velocity responses of the plate in terms of the one-third octave frequency band are obtained for micro-vibration evaluation. Finally, numerical results are given to illustrate the large response reduction capacity of the MRVE sandwich plate with supported mass under stochastic support motion excitations, and the influences of MRVE parameters, supported mass and localized magnetic field placement on the micro-vibration response.

Keywords: micro-vibration; stochastic excitation; sandwich plate; magneto-rheological visco-elastomer; root-mean-square velocity response

1. Introduction

In many fields, there exist vibration-sensitive precise apparatuses and facilities which require

*Corresponding author, Ph.D., E-mail: ceyfduan@zju.edu.cn
[a] Professor, E-mail: yingzg@zju.edu.cn
[b] Professor, E-mail: yiqing.ni@polyu.edu.hk

Copyright © 2015 Techno-Press, Ltd.
http://www.techno-press.org/?journal=sss&subpage=8 ISSN: 1738-1584 (Print), 1738-1991 (Online)

extremely high operation stability. For example, to obtain an advanced light source or stable electron beams, a synchrotron radiation facility is required to control its vibration with displacement and acceleration less than several micrometers and millimeters per square second, respectively. This micro-amplitude vibration is called micro-vibration. The vibration-sensitive equipments are disturbed inevitably by actual environments such as vehicle traffic and machine operation, which are in random with wide frequency bands and long time periods. Thus the stochastic micro-vibration control of the vibration-sensitive equipments is a very significant subject (Yang and Agrawal 2000, Nakamura *et al.* 2000, Yoshioka *et al.* 2001, Xu *et al.* 2003, Hwang *et al.* 2003, Lee *et al.* 2013). Generic micro-vibration criteria for the vibration-sensitive equipments have been presented in terms of the root-mean-square velocity spectrum (Gordon 1991, Amick 1997), which differs from the conventional criteria of strong vibration control. The micro-vibration reduction of structures supporting equipments has been studied by using passive and active isolators (Yang and Agrawal 2000, Nakamura *et al.* 2000, Yoshioka *et al.* 2001, Xu *et al.* 2003, Hwang *et al.* 2003). However, the practical effectiveness of the vibration control using several supplemental devices will be restricted by point energy dissipation and micro-vibration uncertainty. Smart composite structures with area energy dissipation can effectively reduce the stochastic micro-vibration (Ying and Ni 2009, Ni *et al.* 2011).

Magneto-rheological visco-elastomer (MRVE) is a promising smart material, which is fabricated generally by magnetically polarizable iron particles, non-magnetic silicone rubber and silicone oil (Shiga and Okada 1995, Carlson and Jolly 2000). The MRVE improves the potential disadvantage of magnetic particle settlement in magneto-rheological fluids, and combines the advantageous properties of magneto-rheological fluid devices (Dyke *et al.* 1996, Symans and Constantinou 1999, Spencer and Nagarajaiah 2003, Wang and Liao 2011, Casciati *et al.* 2012, Guan 2012) and viscoelastic substrate materials. For example, the MRVE stiffness and damping can be changed reversibly in milliseconds under applied magnetic fields. Many studies have been presented on the MRVE fabrication and test for magnetic mechanical properties and dynamic behaviors (Ginder *et al.* 2002, Bellan and Bossis 2002, Demchuk and Kuz'min 2002, Shen *et al.* 2004, Nikitin and Samus 2005, Gong *et al.* 2005, Böse 2007, Kallio *et al.* 2007, Koo *et al.* 2010, Ying *et al.* 2013). The static modeling for the MRVE shear modulus under applied magnetic fields was given based on the magnetic dipole interaction and polymeric nonlinear elasticity. A complex shear modulus was proposed for describing the MRVE dynamic characteristics under applied magnetic fields based on the polymer dynamics in the frequency domain. The MRVE nonlinear dynamic model and equivalent linear model in the frequency domain for the micro-vibration were also proposed. The MRVE based tunable vibration isolators, absorbers and dampers, and tunable magneto-rheological fluid-elastomer composite dampers and isolators have been designed and tested for strong vibration controls (York *et al.* 2007, Hu and Wereley 2008, Hoang *et al.* 2011, Jung *et al.* 2011).

For another potential application, the MRVE can be used as smart cores to construct composite structures with controllable dynamic characteristics, and then structural vibration can be controlled effectively. Sandwich beams and plates are typical composite structures. Their vibration with uncontrollable viscoelastic damping has been studied early (Ditaranto 1965, Mead and Markus 1969, Yan and Dowell 1972, Mead 1972, Frostig and Baruch 1994). The recent study on MRVE sandwich beams has been presented including the periodic vibration and adjustable stiffness (Zhou and Wang 2005, 2006); frequency-response characteristics (Choi *et al.* 2010); periodic vibration analysis using the finite element method (Nayak *et al.* 2013); dynamic stability under periodic axial loads (Dwivedy *et al.* 2009) and micro-vibration responses (Ying and Ni 2009, Ni *et al.*

2011). The vibration control of piezoelectric composite structures has also been studied (Schoeftner and Buchberger 2013, Zenz *et al.* 2013). Only several studies on MRVE sandwich plate dynamics have been presented (Ying *et al.* 2014). For example, the harmonic acoustic wave transmission characteristics of an infinite MRVE sandwich plate have been analyzed (Hasheminejad and Shabanimotlagh 2010), and the modal frequencies and damping of an MRVE sandwich plate have been calculated by using the finite element method (Yeh 2013). However, the controlled mass such as the vibration-sensitive equipment supported on a composite structure needs to be taken into account for the micro-vibration control. The stochastic vibration reduction of the composite structure under localized magnetic fields needs to be considered for an actual magnetic field covering incompletely large structure. Thus the stochastic micro-vibration suppression capability of the MRVE sandwich plate with supported mass under a localized magnetic field needs to be studied further.

In this paper, the stochastic micro-vibration response of a sandwich plate with MRVE core and supported mass under stochastic support motion excitations is studied and the micro-vibration suppression capability of the sandwich plate is evaluated. The effects of the supported mass and localized magnetic field on the stochastic micro-vibration response of the MRVE sandwich plate are taken into account. A frequency-domain solution method for the stochastic micro-vibration response is developed. Firstly, the basic assumptions for the MRVE sandwich plate are given, and the dynamic characteristics of the MRVE core in micro-vibration are described by a complex modulus dependent on vibration frequency and controllable by applied magnetic fields. The partial differential equations for coupled transverse and longitudinal motions of the MRVE sandwich plate with supported mass are derived based on the dynamic equilibrium, constitutive and geometric relations. Secondly, the displacements of the MRVE sandwich plate are expanded as series in space, and the Galerkin method is used to convert the partial differential equations into ordinary differential equations. The equations are simplified further to those only for the transverse motion of the MRVE sandwich plate with supported mass under the localized magnetic field. Then based on the random vibration theory, the frequency-response function and response power spectral density matrices of the plate system are derived. The root-mean-square velocity response expression of the MRVE sandwich plate with supported mass in terms of the one-third octave frequency band is obtained as the micro-vibration criterion. Finally, numerical results are given on the root-mean-square velocity response spectrum, and the effects of sandwich plate parameters, supported mass and localized magnetic field on the micro-vibration response. The micro-vibration suppression capability of the MRVE sandwich plate with supported mass under stochastic support motion excitations is evaluated.

2. Vibration equations of MRVE sandwich plate with supported mass

Consider a sandwich plate with controllable MRVE core and a supported concentrated mass as shown in Fig. 1. The sandwich plate is subjected to stochastic support micro-motion excitations and the micro-vibration of the plate or supported mass can be controlled by the MRVE core under various magnetic fields. The length and width of the sandwich plate are a and b, respectively. The two facial layers are the linearly elastic material and have the identical elastic modulus of E_1, Poisson's ratio of μ, mass density of ρ_1 and thickness of h_1. The MRVE core layer is soft relative to the facial layers and has the complex shear modulus of G_2, mass density of ρ_2 and thickness of h_2. The supports have the vertical displacement w_0, which is a stochastic micro-motion excitation.

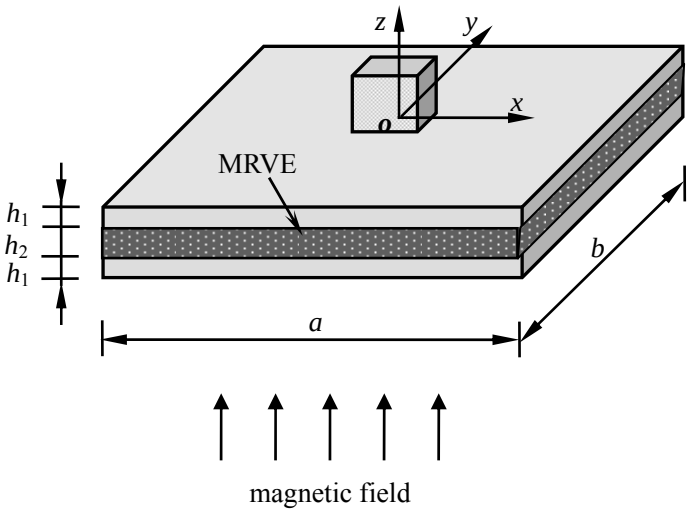

Fig. 1 Sandwich plate with MRVE core

The supported mass is fixed on the plate and has the mass per unit area of m, which volume is small relative to the plate and can be neglected. The facial layers are a non-magnetic material and the core layer is the magnetically controlled material. The localized magnetic field is considered so that the complex modulus of the MRVE core varies with applying region. The magnetic field of intensity B_{m} is applied vertically with the center of ($x_{0\mathrm{m}}$, $y_{0\mathrm{m}}$) and length-width of (a_{m}, b_{m}). Then the complex modulus G_2 becomes $G_{2\mathrm{m}}(B_{\mathrm{m}})$ for the region covered by the localized magnetic field.

The MRVE has the stiffness and damping controllable by applied magnetic fields. Its shear strain depends linearly on the applied shear stress for small deformation. Its dynamic behavior or stress-strain relationship can be described by using the complex modulus dependent on vibration frequency and controllable by applied magnetic fields (Ying *et al.* 2013). The shearing dynamic model of the MRVE in micro-vibration is

$$\tau_2 = G_2(\mathrm{j}\omega, B_{\mathrm{m}})\gamma_2 \tag{1}$$

where τ_2 and γ_2 are respectively the shear stress and shear strain; ω is the vibration frequency and $\mathrm{j}=\sqrt{-1}$. The complex modulus is the function of vibration frequency and applied magnetic field intensity, and can be expressed by separating real part and imaginary part as

$$G_2(\mathrm{j}\omega, B_{\mathrm{m}}) = G^{\mathrm{R}}(\omega, B_{\mathrm{m}})[1+\mathrm{j}\Delta(\omega, B_{\mathrm{m}})] \tag{2}$$

where the real part G^{R} is called the storage modulus representing the MRVE stiffness; the imaginary part $G^{\mathrm{R}}\Delta$ is called the loss modulus; and Δ is called the loss factor representing the MRVE damping. In micro-vibration with frequency less than certain value, the storage modulus and loss factor are approximately $G^{\mathrm{R}}=\alpha_0+\alpha_1\omega$ and $\Delta=\beta_0$, where coefficients α_0, α_1 and β_0 only depend on applied magnetic fields (Ying *et al.* 2013).

For the sandwich plate, it is assumed that: (1) the two elastic facial layers and MRVE core layer are respectively homogeneous and continuous; and the facial layer materials are isotropic while the core material is transversely isotropic under an applied magnetic field along the *z*-axis; (2) the normal stress of the core layer is relatively small and neglected; (3) the normal stresses of the facial layers in the direction of *z*-axis are relatively small and neglected; (4) the vertical displacement of the sandwich plate is invariant along the thickness; (5) the cross section of each facial layer is perpendicular to its axis line in deformation; and the cross section of the core layer is a plane in deformation; (6) the longitudinal and rotational inertias of the plate are relatively small and neglected; (7) the interfaces between the facial layers and core layer are continuous all the time (Ni *et al.* 2011, Yan and Dowell 1972, Mead 1972).

Based on the above assumptions, the displacements and stresses on the interfaces between the facial layers and core layer are continuous. The vertical displacement of the sandwich plate relative to the supports is $w=w(x, y, t)$. The horizontal displacements of the lower and upper facial layers along the *x*-axis and *y*-axis are expressed respectively as

$$u_1(x, y, z_1, t) = u_{10}(x, y, t) - z_1 \frac{\partial w(x, y, t)}{\partial x} \tag{3a}$$

$$v_1(x, y, z_1, t) = v_{10}(x, y, t) - z_1 \frac{\partial w(x, y, t)}{\partial y} \tag{3b}$$

$$u_3(x, y, z_3, t) = u_{30}(x, y, t) - z_3 \frac{\partial w(x, y, t)}{\partial x} \tag{4a}$$

$$v_3(x, y, z_3, t) = v_{30}(x, y, t) - z_3 \frac{\partial w(x, y, t)}{\partial y} \tag{4b}$$

where u_{10}, v_{10}, u_{30} and v_{30} are respectively the mid-layer displacements of the lower and upper facial layers; z_1 and z_3 are the local transverse coordinates of the two facial layers. The horizontal normal strains and shear strains of the facial layers can be obtained by using the geometric relations with displacements (3) and (4). The corresponding normal stresses and shear stresses of the lower and upper facial layers are respectively

$$\sigma_{1x} = \frac{E_1}{1-\mu^2}\left(\frac{\partial u_{10}}{\partial x} + \mu \frac{\partial v_{10}}{\partial y} - z_1 \frac{\partial^2 w}{\partial x^2} - z_1 \mu \frac{\partial^2 w}{\partial y^2}\right) \tag{5a}$$

$$\sigma_{1y} = \frac{E_1}{1-\mu^2}\left(\frac{\partial v_{10}}{\partial y} + \mu \frac{\partial u_{10}}{\partial x} - z_1 \frac{\partial^2 w}{\partial y^2} - z_1 \mu \frac{\partial^2 w}{\partial x^2}\right) \tag{5b}$$

$$\tau_{1xy} = \frac{E_1}{2(1+\mu)}\left(\frac{\partial u_{10}}{\partial y} + \frac{\partial v_{10}}{\partial x} - 2z_1 \frac{\partial^2 w}{\partial x \partial y}\right) \tag{5c}$$

$$\sigma_{3x} = \frac{E_1}{1-\mu^2}\left(\frac{\partial u_{30}}{\partial x} + \mu\frac{\partial v_{30}}{\partial y} - z_3\frac{\partial^2 w}{\partial x^2} - z_3\mu\frac{\partial^2 w}{\partial y^2}\right) \tag{6a}$$

$$\sigma_{3y} = \frac{E_1}{1-\mu^2}\left(\frac{\partial v_{30}}{\partial y} + \mu\frac{\partial u_{30}}{\partial x} - z_3\frac{\partial^2 w}{\partial y^2} - z_3\mu\frac{\partial^2 w}{\partial x^2}\right) \tag{6b}$$

$$\tau_{3xy} = \frac{E_1}{2(1+\mu)}\left(\frac{\partial u_{30}}{\partial y} + \frac{\partial v_{30}}{\partial x} - 2z_3\frac{\partial^2 w}{\partial x\partial y}\right) \tag{6c}$$

By using the equilibrium conditions in the directions of *x*-axis and *y*-axis, the other shear stresses of the lower and upper facial layers are obtained as

$$\begin{aligned}\tau_{1xz} = &-\frac{E_1}{1-\mu^2}\left[\left(\frac{h_1}{2}+z_1\right)\left(\frac{\partial^2 u_{10}}{\partial x^2}+\mu\frac{\partial^2 v_{10}}{\partial x\partial y}\right)+\left(\frac{h_1^2}{8}-\frac{z_1^2}{2}\right)\left(\frac{\partial^3 w}{\partial x^3}+\mu\frac{\partial^3 w}{\partial x\partial y^2}\right)\right]\\ &-\frac{E_1}{2(1+\mu)}\left[\left(\frac{h_1}{2}+z_1\right)\left(\frac{\partial^2 u_{10}}{\partial y^2}+\frac{\partial^2 v_{10}}{\partial x\partial y}\right)+\left(\frac{h_1^2}{4}-z_1^2\right)\frac{\partial^3 w}{\partial x\partial y^2}\right]\end{aligned} \tag{7a}$$

$$\begin{aligned}\tau_{1yz} = &-\frac{E_1}{1-\mu^2}\left[\left(\frac{h_1}{2}+z_1\right)\left(\frac{\partial^2 v_{10}}{\partial y^2}+\mu\frac{\partial^2 u_{10}}{\partial x\partial y}\right)+\left(\frac{h_1^2}{8}-\frac{z_1^2}{2}\right)\left(\frac{\partial^3 w}{\partial y^3}+\mu\frac{\partial^3 w}{\partial x^2\partial y}\right)\right]\\ &-\frac{E_1}{2(1+\mu)}\left[\left(\frac{h_1}{2}+z_1\right)\left(\frac{\partial^2 v_{10}}{\partial x^2}+\frac{\partial^2 u_{10}}{\partial x\partial y}\right)+\left(\frac{h_1^2}{4}-z_1^2\right)\frac{\partial^3 w}{\partial x^2\partial y}\right]\end{aligned} \tag{7b}$$

$$\begin{aligned}\tau_{3xz} = &\frac{E_1}{1-\mu^2}\left[\left(\frac{h_1}{2}-z_3\right)\left(\frac{\partial^2 u_{30}}{\partial x^2}+\mu\frac{\partial^2 v_{30}}{\partial x\partial y}\right)-\left(\frac{h_1^2}{8}-\frac{z_3^2}{2}\right)\left(\frac{\partial^3 w}{\partial x^3}+\mu\frac{\partial^3 w}{\partial x\partial y^2}\right)\right]\\ &+\frac{E_1}{2(1+\mu)}\left[\left(\frac{h_1}{2}-z_3\right)\left(\frac{\partial^2 u_{30}}{\partial y^2}+\frac{\partial^2 v_{30}}{\partial x\partial y}\right)-\left(\frac{h_1^2}{4}-z_3^2\right)\frac{\partial^3 w}{\partial x\partial y^2}\right]\end{aligned} \tag{8a}$$

$$\begin{aligned}\tau_{3yz} = &\frac{E_1}{1-\mu^2}\left[\left(\frac{h_1}{2}-z_3\right)\left(\frac{\partial^2 v_{30}}{\partial y^2}+\mu\frac{\partial^2 u_{30}}{\partial x\partial y}\right)-\left(\frac{h_1^2}{8}-\frac{z_3^2}{2}\right)\left(\frac{\partial^3 w}{\partial y^3}+\mu\frac{\partial^3 w}{\partial x^2\partial y}\right)\right]\\ &+\frac{E_1}{2(1+\mu)}\left[\left(\frac{h_1}{2}-z_3\right)\left(\frac{\partial^2 v_{30}}{\partial x^2}+\frac{\partial^2 u_{30}}{\partial x\partial y}\right)-\left(\frac{h_1^2}{4}-z_3^2\right)\frac{\partial^3 w}{\partial x^2\partial y}\right]\end{aligned} \tag{8b}$$

Based on the above assumptions, the cross section of the MRVE core layer is a plane in deformation. By using the displacements on the two interfaces of the sandwich plate, the shear strains of the core are obtained as

$$\gamma_{xz} = \frac{h_s}{h_2}\frac{\partial w}{\partial x} + \frac{u_{30}-u_{10}}{h_2}, \quad \gamma_{yz} = \frac{h_s}{h_2}\frac{\partial w}{\partial y} + \frac{v_{30}-v_{10}}{h_2} \tag{9a,b}$$

where $h_s=h_1+h_2$. According to the dynamic model (1) with the complex modulus $G_2(\mathrm{j}\omega, B_\mathrm{m})$, the shear stresses of the MRVE core are

$$\tau_{xz}=G_2\left(\frac{h_s}{h_2}\frac{\partial w}{\partial x}+\frac{u_{30}-u_{10}}{h_2}\right),\quad \tau_{yz}=G_2\left(\frac{h_s}{h_2}\frac{\partial w}{\partial y}+\frac{v_{30}-v_{10}}{h_2}\right) \tag{10a,b}$$

Based on the continuity conditions of shear stresses on the interfaces between the facial layers and core layer, the differential equations for the horizontal displacements of the facial layers are obtained as

$$\frac{E_1}{1-\mu^2}\frac{\partial^2 u}{\partial x^2}+\frac{E_1}{2(1+\mu)}\frac{\partial^2 u}{\partial y^2}-\frac{2G_2 u}{h_1 h_2}+\frac{E_1}{2(1-\mu)}\frac{\partial^2 v}{\partial x\partial y}+\frac{G_2 h_s}{h_1 h_2}\frac{\partial w}{\partial x}=0 \tag{11}$$

$$\frac{E_1}{2(1+\mu)}\frac{\partial^2 v}{\partial x^2}+\frac{E_1}{1-\mu^2}\frac{\partial^2 v}{\partial y^2}-\frac{2G_2 v}{h_1 h_2}+\frac{E_1}{2(1-\mu)}\frac{\partial^2 u}{\partial x\partial y}+\frac{G_2 h_s}{h_1 h_2}\frac{\partial w}{\partial y}=0 \tag{12}$$

where $u=u_{10}=-u_{30}$ and $v=v_{10}=-v_{30}$. The dynamic equilibrium equation of each element of the sandwich plate with the supported concentrated mass in the direction of z-axis is

$$\int_{2h_1+h_2}\left(\frac{\partial \tau_{xz}}{\partial x}+\frac{\partial \tau_{yz}}{\partial y}\right)\mathrm{d}z=[\rho_a h_t+mab\delta(x-x_{\mathrm{sm}})\delta(y-y_{\mathrm{sm}})](\ddot{w}+\ddot{w}_0) \tag{13}$$

where $\ddot{w}_0$ is the stochastic support acceleration of vertical micro-motion; $\delta(\cdot)$ is the Dirac delta function; $(x_{\mathrm{sm}}, y_{\mathrm{sm}})$ are the coordinates of the mass in plane (x, y); $\rho_a h_t=2\rho_1 h_1+\rho_2 h_2$ and $h_t=2h_1+h_2$. Substituting the shear stress expressions (7), (8) and (10) into Eq. (13) yields the following differential equation for the vertical displacement of the plate

$$[\rho_a h_t+mab\delta(x-x_{\mathrm{sm}})\delta(y-y_{\mathrm{sm}})](\ddot{w}+\ddot{w}_0)+D_1\nabla^4 w-\frac{G_2 h_s}{h_2}\left[h_s\nabla^2 w-2\left(\frac{\partial u}{\partial x}+\frac{\partial v}{\partial y}\right)\right]=0 \tag{14}$$

where $D_1=E_1 h_1^3/6(1-\mu^2)$ and $\nabla^2=\partial^2/\partial x^2+\partial^2/\partial y^2$. The partial differential Eqs. (11), (12) and (14) describe the coupled transverse and longitudinal vibrations of the MRVE sandwich plate with supported mass under support motion excitations. In the case of the localized magnetic field, the complex modulus G_2 of the MRVE core is the function of x and y, determined by the magnetic field distribution. For the simply supported rectangular plate, the boundary conditions obtained are (Mead and Markus 1969, Ying *et al.* 2014)

$$w\big|_{x=\pm a/2}=0,\ w\big|_{y=\pm b/2}=0,\ \frac{\partial^2 w}{\partial x^2}\Big|_{x=\pm a/2}=0,\ \frac{\partial^2 w}{\partial y^2}\Big|_{y=\pm b/2}=0,$$

$$\left(\frac{\partial u}{\partial x}+\mu\frac{\partial v}{\partial y}\right)\Big|_{x=\pm a/2}=0,\ \left(\frac{\partial v}{\partial y}+\mu\frac{\partial u}{\partial x}\right)\Big|_{y=\pm b/2}=0 \tag{15}$$

The vibration Eqs. (14), (11) and (12) with the boundary conditions (15) can be rewritten in the dimensionless form as follows

$$[\rho_a h_t + m\delta(\bar{x}-\bar{x}_{\rm sm})\delta(\bar{y}-\bar{y}_{\rm sm})](\ddot{\bar{w}}+\ddot{\bar{w}}_0) + D_1(\frac{\partial^4\bar{w}}{a^4\partial\bar{x}^4}+\frac{2}{a^2b^2}\frac{\partial^4\bar{w}}{\partial\bar{x}^2\partial\bar{y}^2}+\frac{\partial^4\bar{w}}{b^4\partial\bar{y}^4}) - \frac{G_2h_s}{h_2}[h_s(\frac{\partial^2\bar{w}}{a^2\partial\bar{x}^2}+\frac{\partial^2\bar{w}}{b^2\partial\bar{y}^2})-2(\frac{\partial\bar{u}}{a\partial\bar{x}}+\frac{\partial\bar{v}}{b\partial\bar{y}})]=0 \tag{16}$$

$$\frac{E_1}{1-\mu^2}\frac{\partial^2\bar{u}}{a^2\partial\bar{x}^2}+\frac{E_1}{2(1+\mu)}\frac{\partial^2\bar{u}}{b^2\partial\bar{y}^2}-\frac{2G_2\bar{u}}{h_1h_2}+\frac{E_1}{2(1-\mu)}\frac{\partial^2\bar{v}}{ab\partial\bar{x}\partial\bar{y}}+\frac{G_2h_s}{h_1h_2}\frac{\partial\bar{w}}{a\partial\bar{x}}=0 \tag{17}$$

$$\frac{E_1}{2(1+\mu)}\frac{\partial^2\bar{v}}{a^2\partial\bar{x}^2}+\frac{E_1}{1-\mu^2}\frac{\partial^2\bar{v}}{b^2\partial\bar{y}^2}-\frac{2G_2\bar{v}}{h_1h_2}+\frac{E_1}{2(1-\mu)}\frac{\partial^2\bar{u}}{ab\partial x\partial y}+\frac{G_2h_s}{h_1h_2}\frac{\partial\bar{w}}{b\partial\bar{y}}=0 \tag{18}$$

$$\bar{w}\big|_{\bar{x}=\pm1/2}=0,\ \bar{w}\big|_{\bar{y}=\pm1/2}=0,\ \frac{\partial^2\bar{w}}{\partial\bar{x}^2}\big|_{\bar{x}=\pm1/2}=0,\ \frac{\partial^2\bar{w}}{\partial\bar{y}^2}\big|_{\bar{y}=\pm1/2}=0,$$

$$(\frac{\partial\bar{u}}{a\partial\bar{x}}+\mu\frac{\partial\bar{v}}{b\partial\bar{y}})\big|_{\bar{x}=\pm1/2}=0,\ (\frac{\partial\bar{v}}{b\partial\bar{y}}+\mu\frac{\partial\bar{u}}{a\partial\bar{x}})\big|_{\bar{y}=\pm1/2}=0 \tag{19}$$

where the amplitude of the support motion w_0 is W_a; and the dimensionless coordinates and displacements are

$$\bar{x}=\frac{x}{a},\ \bar{y}=\frac{y}{b},\ \bar{u}=\frac{u}{W_a},\ \bar{v}=\frac{v}{W_a},\ \bar{w}=\frac{w}{W_a},\ \bar{w}_0=\frac{w_0}{W_a} \tag{20}$$

3. Stochastic micro-vibration solution of MRVE sandwich plate with supported mass

Under the homogeneous boundary conditions (19), the vibration displacements of the MRVE sandwich plate with supported mass can be expanded in harmonic functions as (Mead 1972)

$$\bar{w}=\sum_{i=1}^{N_1}\sum_{j=1}^{N_2}q_{ij}(t)U_{ic}(\bar{x})V_{jc}(\bar{y}),\quad \bar{u}=\sum_{i=1}^{N_1}\sum_{j=1}^{N_2}r_{ij}(t)U_{is}(\bar{x})V_{jc}(\bar{y}),\quad \bar{v}=\sum_{i=1}^{N_1}\sum_{j=1}^{N_2}s_{ij}(t)U_{ic}(\bar{x})V_{js}(\bar{y}) \tag{21}$$

$$U_{is}(\bar{x})=\sin(2i-1)\pi\bar{x},\quad U_{ic}(\bar{x})=\cos(2i-1)\pi\bar{x},$$

$$V_{js}(\bar{y}) = \sin(2j-1)\pi\bar{y}, \quad V_{jc}(\bar{y}) = \cos(2j-1)\pi\bar{y} \tag{22}$$

where $q_{ij}(t)$, $r_{ij}(t)$ and $s_{ij}(t)$ are functions of time; N_1 and N_2 are integers. According to the Galerkin method, substituting displacements (21) into Eqs. (16)-(18), multiplying the equations respectively by $U_{kc}V_{lc}$, $U_{ks}V_{lc}$, $U_{kc}V_{ls}$, and integrating them with respect to $\bar{x}$ and $\bar{y}$ yield ordinary differential equations for q_{ij} and algebraic equations for r_{ij} and s_{ij}. By eliminating functions r_{ij} and s_{ij}, the ordinary differential equations for $q_{ij}(t)$ can be obtained and rewritten in the matrix form as

$$\mathbf{M}\ddot{\mathbf{Q}} + \mathbf{K}\mathbf{Q} = \mathbf{F}(t) \tag{23}$$

where the modal displacement vector **Q**, modal excitation vector **F**, modal mass matrix **M** and modal stiffness matrix **K** are

$$\mathbf{Q} = \begin{Bmatrix} \mathbf{Q}_1 \\ \mathbf{Q}_2 \\ \vdots \\ \mathbf{Q}_{N_2} \end{Bmatrix}, \quad \mathbf{Q}_j = \begin{Bmatrix} q_{1j} \\ q_{2j} \\ \vdots \\ q_{N_1 j} \end{Bmatrix}, \quad \mathbf{F} = \ddot{\bar{w}}_0\mathbf{C} \overset{\Delta}{=} \ddot{\bar{w}}_0 \begin{Bmatrix} \mathbf{C}_1 \\ \mathbf{C}_2 \\ \vdots \\ \mathbf{C}_{N_2} \end{Bmatrix}, \quad \mathbf{C}_l = \begin{Bmatrix} c_{1l} \\ c_{2l} \\ \vdots \\ c_{N_1 l} \end{Bmatrix},$$

$$\mathbf{M} = \frac{\rho_a h_t}{4}\mathbf{I} + m[\cos(2i-1)\pi\bar{x}_{\mathrm{sm}}\cos(2j-1)\pi\bar{y}_{\mathrm{sm}}\cos(2k-1)\pi\bar{x}_{\mathrm{sm}}\cos(2l-1)\pi\bar{y}_{\mathrm{sm}}]_{N\times N},$$

$$c_{kl} = \frac{4\rho_a h_t(-1)^{k+l+1}}{\pi^2(2k-1)(2l-1)} - m\cos(2k-1)\pi\bar{x}_{\mathrm{sm}}\cos(2l-1)\pi\bar{y}_{\mathrm{sm}},$$

$$\mathbf{K} = [\mathbf{B}_8 + \mathbf{B}_6(\mathbf{B}_4\mathbf{B}_2^{-1}\mathbf{B}_1 - \mathbf{B}_2)^{-1}(\mathbf{B}_5 - \mathbf{B}_4\mathbf{B}_2^{-1}\mathbf{B}_3) + \mathbf{B}_7(\mathbf{B}_1\mathbf{B}_2^{-1}\mathbf{B}_4 - \mathbf{B}_2)^{-1}(\mathbf{B}_3 - \mathbf{B}_1\mathbf{B}_2^{-1}\mathbf{B}_5)],$$

$$\mathbf{B}_8 = [(a_i^2 + b_j^2)\{\frac{\pi^4 D_1}{4}\delta_{ik}\delta_{jl}(a_i^2 + b_j^2) + \frac{\pi^2 h_s^2}{h_2}b_{3ijkl}\}]_{N\times N}, \quad \mathbf{B}_7 = [\frac{2\pi h_s}{h_2}b_j b_{3ijkl}]_{N\times N},$$

$$\mathbf{B}_6 = [\frac{2\pi h_s}{h_2}a_i b_{3ijkl}]_{N\times N}, \quad \mathbf{B}_5 = [\frac{\pi h_s}{h_1 h_2}b_j b_{2ijkl}]_{N\times N}, \quad \mathbf{B}_2 = [\frac{\pi^2 E_1}{8(1-\mu)}a_i b_j \delta_{ik}\delta_{jl}]_{N\times N},$$

$$\mathbf{B}_3 = [\frac{\pi h_s}{h_1 h_2}a_i b_{1ijkl}]_{N\times N}, \quad \mathbf{B}_4 = [\{\frac{\pi^2 E_1}{8(1+\mu)}a_i^2 + \frac{\pi^2 E_1}{4(1-\mu^2)}b_j^2\}\delta_{ik}\delta_{jl} + \frac{2}{h_1 h_2}b_{2ijkl}]_{N\times N},$$

$$\mathbf{B}_1 = [\{\frac{\pi^2 E_1}{4(1-\mu^2)}a_i^2 + \frac{\pi^2 E_1}{8(1+\mu)}b_j^2\}\delta_{ik}\delta_{jl} + \frac{2}{h_1 h_2}b_{1ijkl}]_{N\times N},$$

$$a_i = \frac{2i-1}{a}, \quad b_j = \frac{2j-1}{b}, \quad \delta_{ik} = \begin{cases} 1 & i = k \\ 0 & i \neq k \end{cases}, \quad \delta_{jl} = \begin{cases} 1 & j = l \\ 0 & j \neq l \end{cases},$$

$$b_{1ijkl} = \int\int_{-1/2}^{1/2} G_2 U_{is}(\bar{x}) U_{ks}(\bar{x}) V_{jc}(\bar{y}) V_{lc}(\bar{y}) \mathrm{d}\bar{x}\mathrm{d}\bar{y},$$

$$b_{2ijkl} = \int\int_{-1/2}^{1/2} G_2 U_{ic}(\bar{x}) U_{kc}(\bar{x}) V_{js}(\bar{y}) V_{ls}(\bar{y}) \mathrm{d}\bar{x}\mathrm{d}\bar{y},$$

$$b_{3ijkl} = \int\int_{-1/2}^{1/2} G_2 U_{ic}(\bar{x}) U_{kc}(\bar{x}) V_{jc}(\bar{y}) V_{lc}(\bar{y}) \mathrm{d}\bar{x}\mathrm{d}\bar{y},$$

$$i, k = 1, 2, \ldots, N_1, \quad j, l = 1, 2, \ldots, N_2 \tag{24}$$

in which **I** is the N-dimensional identity matrix; $N=N_1\times N_2$; $G_2=G_{2\mathrm{m}}[\mathrm{j}\omega, B_{\mathrm{m}}(x,y)]$ for the region covered by the localized magnetic field and $G_2=G_{2\mathrm{m}}(\mathrm{j}\omega, 0)$ for the other region. The stiffness **K** is a complex matrix and controlled by the applied magnetic field due to the MRVE core with modulus G_2.

The stochastic environment micro-motion such as train-induced disturbance can be described by an evolutionary spectral density which is obtained approximately by the output of a filtering system with the input of slowly modulated white noise. The equivalent quasi-stationary spectral density can be derived from the filtering system. The spectral density is used for the stochastic support micro-motion excitation of the sandwich plate, which is expressed as (Yang and Agrawal 2000, Ni *et al.* 2011)

$$S_{\ddot{\bar{w}}_0}(\omega) = \psi(\omega) S_g(\omega),$$

$$S_g(\omega) = \frac{s_0^2[1+4\zeta_{g1}^2(\omega/\omega_{g1})^2](\omega/\omega_{g2})^2}{\{[1-(\omega/\omega_{g1})^2]^2+4\zeta_{g1}^2(\omega/\omega_{g1})^2\}\{[1-(\omega/\omega_{g2})^2]^2+4\zeta_{g2}^2(\omega/\omega_{g2})^2\}},$$

$$\psi(\omega) = \frac{2}{\omega^2}\{1+\lambda_{g1}\omega+\lambda_{g2}\omega[\frac{1-\cos\omega t_1}{t_1^2}+\frac{1-\cos\omega(t_3-t_2)}{(t_3-t_2)^2} + \frac{-\cos\omega t_2+\cos\omega t_3+\cos\omega(t_2-t_1)-\cos\omega(t_3-t_1)}{t_1(t_3-t_2)}]\} \tag{25}$$

where t_1, t_2, t_3, λ_{g1}, λ_{g2}, s_0, ω_{g1}, ω_{g2}, ζ_{g1} and ζ_{g2} are constants.

Eq. (23) represents a stochastically excited multi-degree-of-freedom system derived from the MRVE sandwich plate with supported mass, which has the complex stiffness **K** dependent on vibration frequency and controllable by applied magnetic fields. The stochastic micro-vibration response of the plate system can be estimated by using its power spectral density function. The frequency-response function matrix **H** and then the power spectral density matrix $\mathbf{S_Q}$ of the system response obtained are (Ni *et al.* 2011)

$$\mathbf{H}(\omega) = (\mathbf{K} - \omega^2\mathbf{M})^{-1} \tag{26}$$

$$\mathbf{S}_{\mathbf{Q}}(\omega) = \mathbf{H}(\omega)\mathbf{S}_{\mathbf{F}}(\omega)\mathbf{H}^{*\mathrm{T}}(\omega) \tag{27}$$

$$\mathbf{S}_{\mathbf{F}}(\omega) = S_{\ddot{\overline{w}}_0}(\omega)\mathbf{C}\mathbf{C}^{\mathrm{T}} \tag{28}$$

where the superscript * denotes the complex conjugate; and $\mathbf{S}_{\mathbf{F}}$ is the power spectral density matrix of the stochastic excitation $\mathbf{F}$. By using expressions (21) and (27), the response spectrum of vertical displacement of the sandwich plate relative to the supports is obtained as

$$S_{\overline{w}}(\omega, \overline{x}, \overline{y}) = \mathbf{\Phi}^{\mathrm{T}}(\overline{x}, \overline{y})\mathbf{S}_{\mathbf{Q}}(\omega)\mathbf{\Phi}(\overline{x}, \overline{y}) \tag{29}$$

$$\mathbf{\Phi}(\overline{x}, \overline{y}) = [\mathbf{\Phi}_1, \mathbf{\Phi}_2, \cdots, \mathbf{\Phi}_{N_2}]^{\mathrm{T}}, \quad \mathbf{\Phi}_j = [U_{1\mathrm{c}}V_{j\mathrm{c}}, U_{2\mathrm{c}}V_{j\mathrm{c}}, \cdots, U_{N_1\mathrm{c}}V_{j\mathrm{c}}]^{\mathrm{T}} \tag{30}$$

The absolute displacement is $\overline{w}_a = \overline{w} + \overline{w}_0$. The response spectrum of absolute vertical displacement of the sandwich plate is further obtained as

$$S_{\overline{w}_a}(\omega, \overline{x}, \overline{y}) = S_{\overline{w}}(\omega, \overline{x}, \overline{y}) + \mathbf{\Phi}^{\mathrm{T}}(\overline{x}, \overline{y})[\mathbf{S}_{\mathbf{Q}\overline{w}_0}(\omega) + \mathbf{S}^*_{\mathbf{Q}\overline{w}_0}(\omega)] + S_{\overline{w}_0}(\omega) \tag{31}$$

where the spectrum vector $\mathbf{S}^*_{\mathbf{Q}\overline{w}_0}$ is the complex conjugate of $\mathbf{S}_{\mathbf{Q}\overline{w}_0}$; and $\mathbf{S}_{\mathbf{Q}\overline{w}_0}$ is the cross power spectral density vector of the system response and support motion excitation. The corresponding absolute velocity response spectrum of the sandwich plate is

$$S_{\dot{\overline{w}}_a}(\omega, \overline{x}, \overline{y}) = \omega^2 S_{\overline{w}}(\omega, \overline{x}, \overline{y}) - \mathbf{\Phi}^{\mathrm{T}}(\overline{x}, \overline{y})[\mathbf{H}(\omega)\mathbf{C} + \mathbf{H}^*(\omega)\mathbf{C}]S_{\ddot{\overline{w}}_0}(\omega) + \frac{1}{\omega^2} S_{\ddot{\overline{w}}_0}(\omega) \tag{32}$$

Then the stochastic micro-vibration response of the sandwich plate and supported mass can be estimated. For example, the absolute velocity response spectrum at the midpoint of the sandwich plate can be calculated by Eq. (32) with $\overline{x} = \overline{y} = 0$.

In terms of the one-third octave frequency spectrum for micro-vibration (Gordon 1991, Amick 1997), the root-mean-square velocity response of the sandwich plate is expressed as (Ying and Ni 2009, Ni *et al.* 2011)

$$RMS_V(f_c, x, y) = [\int_{f_l}^{f_u} S_{\dot{\overline{w}}_a}(2\pi f, \overline{x}, \overline{y})\mathrm{d}f]^{1/2} \tag{33}$$

where $f_c = \omega_c/2\pi$ is the center frequency of the one-third octave frequency band with the lower limit $f_l = 0.89f_c$ and upper limit $f_u = 1.12f_c$. For the velocity in the unit of μm/s, the logarithmic root-mean-square velocity response is given by

$$LRMS_V(f_c, x, y) = 20\log_{10}[RMS_V(f_c, x, y)] + 120 \tag{34}$$

The root-mean-square velocity response spectrum (33) or (34) is the principal micro-vibration criterion for vibration-sensitive precise instruments. In most cases, the allowable root-mean-square velocity is less than 50 dB within the frequency band of [8, 80] Hz (Gordon 1991, Amick 1997).

4. Numerical results on micro-vibration control effectiveness

To show the micro-vibration suppression capacity, consider a sandwich plate with MRVE core and supported mass under stochastic support micro-motion excitation, which has basic parameters as follows: a=4 m, b=3 m, h_1=5 cm, h_2=10 cm, ρ_1=1500 kg/m^3, ρ_2=700 kg/m^3, m=50 kg/m^2, x_{sm}=0, y_{sm}=0, E_1=0.5 GPa, μ=0.3, α_0=0.3 MPa, α_1=0.01 MPa·s, β_0=0.3; s_0=0.03, t_1=5 s, t_2=10 s, t_3=15 s, λ_{g1}=0.3 s, λ_{g2}=0.1 s^3, ω_{g1}=10.8 Hz, ω_{g2}=38 Hz, ζ_{g1}=0.75, ζ_{g2}=0.35. The sandwich plate parameters chosen are based on an actual floor slab and the stochastic excitation parameters chosen are based on an environment micro-motion spectrum (Ni *et al.* 2011, Yang and Agrawal 2000). Fig. 2 shows the power spectral density of the stochastic support micro-motion excitation with the root-mean-square acceleration of 0.0322 m/s^2.

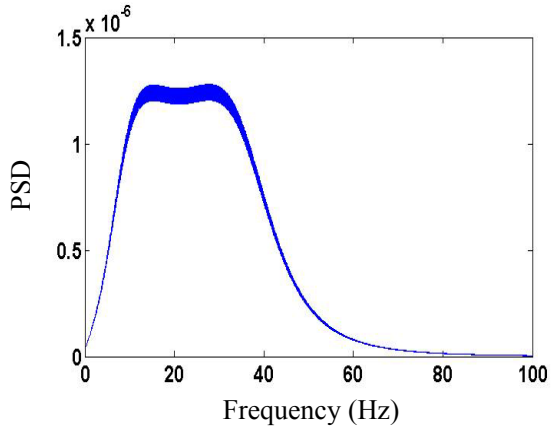

Fig. 2 Power spectral density (PSD) of micro-motion excitation

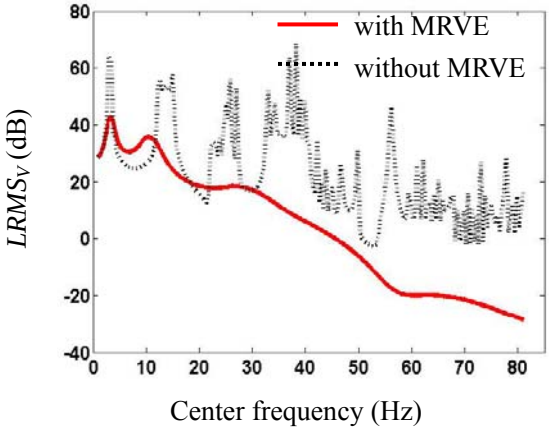

Fig. 3 Logarithmic root-mean-square velocity ($LRMS_v$) spectra of plates with and without MRVE.

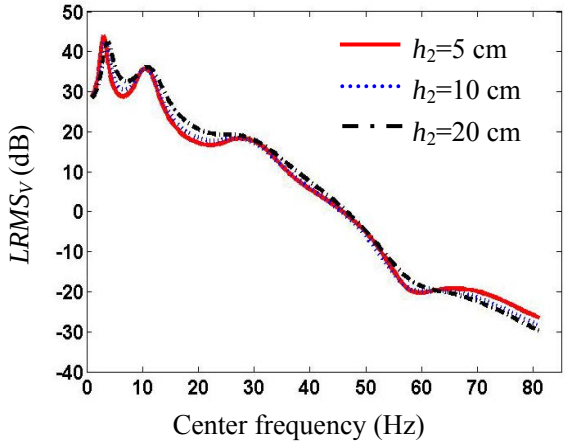

Fig. 4 Logarithmic root-mean-square velocity ($LRMS_v$) spectra of sandwich plate for different thicknesses h_2

Numerical results on the principal micro-vibration criterion, that is the root-mean-square velocity response spectrum of the MRVE sandwich plate with supported mass under various magnetic fields are obtained and shown in Figs. 3-15. Fig. 3 shows the logarithmic root-mean-square velocity response spectrum at the midpoint of the sandwich plate with MRVE under completely covered magnetic field, which is compared with that without MRVE. It is obtained that the micro-vibration response can be greatly reduced by using the MRVE (maximum response from 70 dB to 36 dB with 49% relative reduction in [8, 80] Hz), especially for the center frequency f_c>35 Hz (from 70 dB to 11 dB with 84% relative reduction).

4.1 Micro-vibration responses for various geometric parameters

The influences of the MRVE thickness, plate length and width on the root-mean-square velocity response of the sandwich plate with supported mass under completely covered magnetic field are shown in Figs. 4-7. Fig. 3 illustrates that the root-mean-square velocity response at the midpoint of the MRVE sandwich plate is reduced remarkably for h_2 from 0 to 10 cm (h_2/h_t=1/2) and Fig. 4 illustrates that the root-mean-square velocity response at the midpoint of the MRVE sandwich plate changes slightly for h_2 from 5 cm (h_2/h_t=1/3) to 20 cm (h_2/h_t=2/3).
Then it is obtained that the root-mean-square velocity response of the MRVE sandwich plate is reduced remarkably with the increase of the MRVE thickness h_2 from zero to a small value (for example, 5 cm), and for the thickness larger than the value, the root-mean-square velocity response of the sandwich plate changes slightly with the further increase of the MRVE thickness h_2. Fig. 5 shows the logarithmic root-mean-square velocity response at the midpoint of the MRVE sandwich plate for different length-width ratios b/a under certain length (a=4 m) (maximum responses are 45, 34, 36 dB for b/a=0.3, 0.5, 1, respectively, in [8, 80] Hz). Figs. 6 and 7 illustrate that the logarithmic root-mean-square velocity response at the midpoint of the MRVE sandwich plate varies largely with length a under certain length-width ratio (b/a=0.5, 1) (for example, maximum response from 44 dB [a=2 m] to 24 dB [a=6 m] for b/a=1 in [8, 80] Hz). It is obtained that the root-mean-square velocity response of the MRVE sandwich plate can be reduced for the center

frequency f_c>8 Hz by the increase of the plate length or width, because the increase of the plate length or width results in the modal damping increase and the decreases of the MRVE sandwich plate stiffness and modal frequencies.

4.2 Micro-vibration responses for various MRVE parameters

The influences of the MRVE storage modulus and loss factor on the root-mean-square velocity response of the sandwich plate with supported mass under completely covered magnetic field are then considered. The root-mean-square velocity response at the midpoint of the MRVE sandwich plate changes slightly with the MRVE storage modulus coefficient α_0.

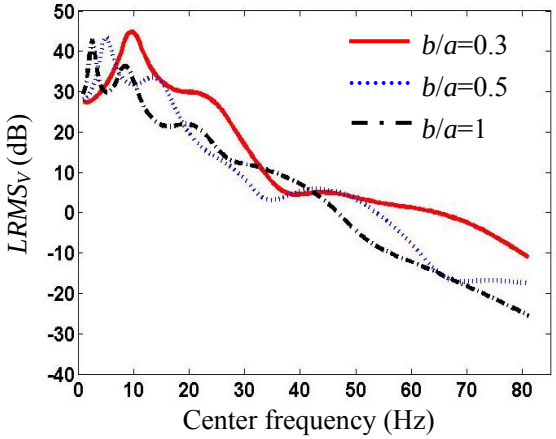

Fig. 5 Logarithmic root-mean-square velocity ($LRMS_v$) spectra of sandwich plate for different length-width ratios b/a (a=4m)

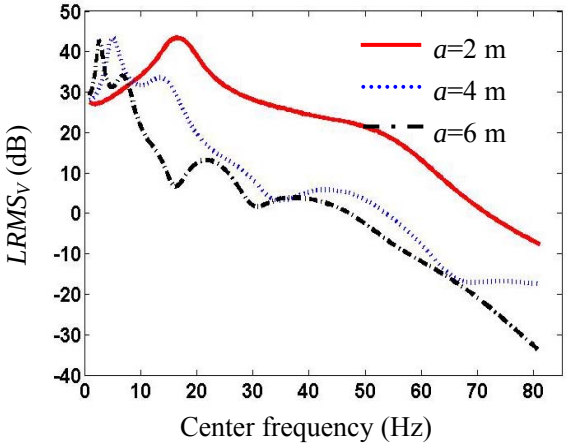

Fig. 6 Logarithmic root-mean-square velocity ($LRMS_v$) spectra of sandwich plate for different lengths a (b/a=0.5)

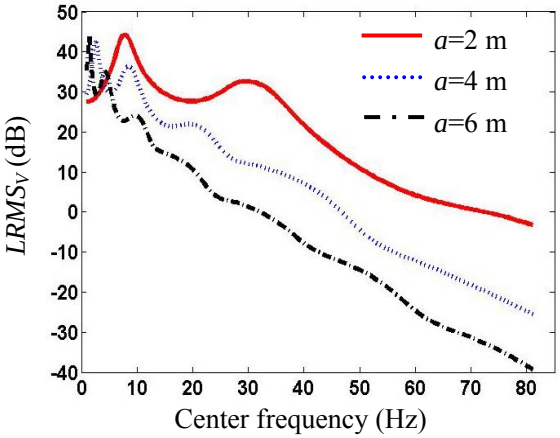

Fig. 7 Logarithmic root-mean-square velocity ($LRMS_v$) spectra of sandwich plate for different lengths a (b/a=1)

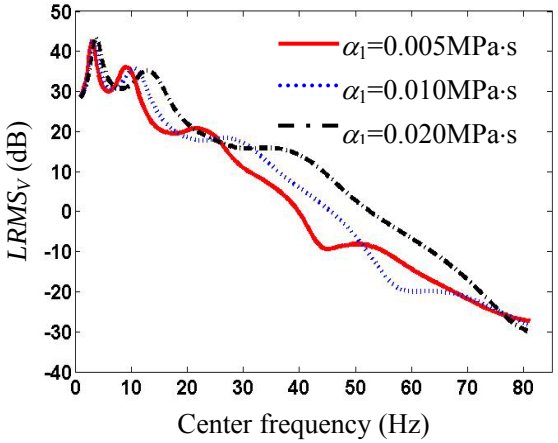

Fig. 8 Logarithmic root-mean-square velocity ($LRMS_v$) spectra of sandwich plate for different values of MRVE storage modulus coefficient α_1

Fig. 8 shows the logarithmic root-mean-square velocity response at the midpoint of the MRVE sandwich plate for different values of the MRVE storage modulus coefficient α_1. The storage modulus coefficient α_1 has complicated effects on the root-mean-square velocity response in the concerned frequency band, because the increase of the frequency-dependent storage modulus coefficient results in the increase of the MRVE sandwich plate stiffness for higher frequency more than lower frequency and the modal frequencies varying correspondingly. Fig. 9 illustrates that the logarithmic root-mean-square velocity response of the MRVE sandwich plate is reduced by the increase of the MRVE loss factor β_0 (maximum response from 39 dB [β_0=0.2] to 31 dB [β_0=0.6] in [8, 80] Hz).

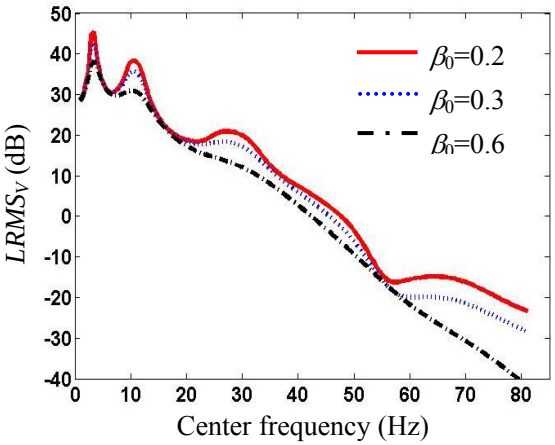

Fig. 9 Logarithmic root-mean-square velocity ($LRMS_v$) spectra of sandwich plate for different values of MRVE loss factor β_0

4.3 Micro-vibration responses for various supported masses and positions

The influences of the concentrated mass supported by the sandwich plate and its position on the root-mean-square velocity response of the MRVE sandwich plate under completely covered magnetic field are shown in Figs. 10-12. Fig. 10 illustrates that the logarithmic root-mean-square velocity response at the midpoint of the MRVE sandwich plate decreases with the increase of the supported mass m for the position of x_{sm}=0 and y_{sm}=0 (in particular, for the center frequency f_c>20 Hz, maximum response from 31 dB [m=10 kg/m^2] to 19 dB [m=50 kg/m^2]), because of the increase of vertical inertia.

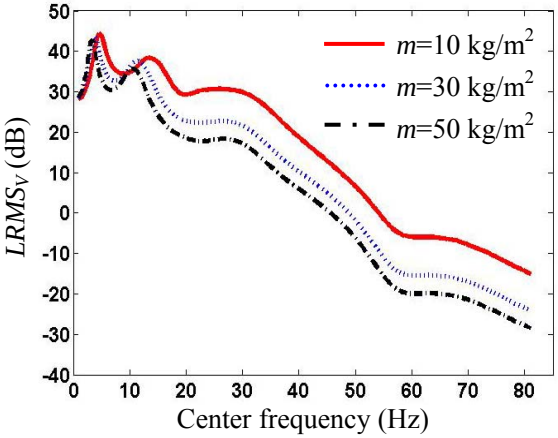

Fig. 10 Logarithmic root-mean-square velocity ($LRMS_v$) spectra of sandwich plate for different values of supported mass m

Fig. 11 shows the logarithmic root-mean-square velocity response at the midpoint (x=0, y=0) of the MRVE sandwich plate for different positions (x_{sm}, y_{sm}) of the supported mass. It is seen that the root-mean-square velocity response of the sandwich plate has the smallest value for the supported mass fixed at the midpoint, in particular, for the center frequency f_c>15 Hz. Fig. 12 shows the logarithmic root-mean-square velocity response at the support point (x=x_{sm}, y=y_{sm}) of the MRVE sandwich plate for different positions (x_{sm}, y_{sm}) of the supported mass (maximum responses are 18, 24, 27, 24 dB for {x_{sm}/a, y_{sm}/b}={0, 0}, {0, 1/4}, {1/4, 0}, {1/4, 1/4}, respectively, and for the center frequency f_c>20 Hz). The root-mean-square velocity response of the support point or supported mass is small relatively for the mass at the midpoint and high frequency.

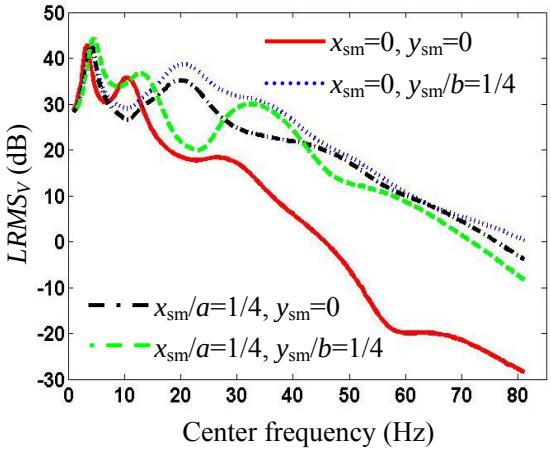

Fig. 11 Logarithmic root-mean-square velocity ($LRMS_v$) spectra of sandwich plate (x=y=0) for different positions of supported mass (x_{sm}, y_{sm})

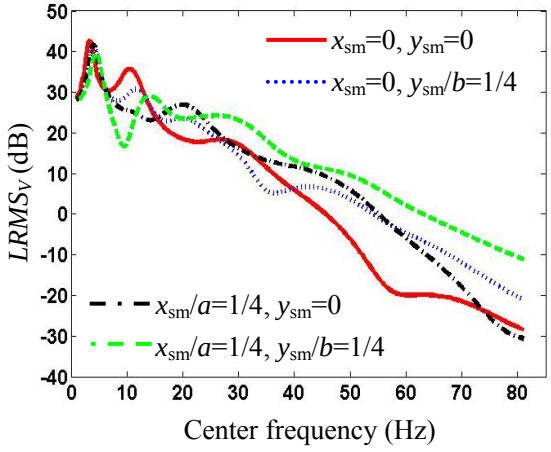

Fig. 12 Logarithmic root-mean-square velocity ($LRMS_v$) spectra of sandwich plate at the support point (x=x_{sm}, y=y_{sm}) for different positions of supported mass (x_{sm}, y_{sm})

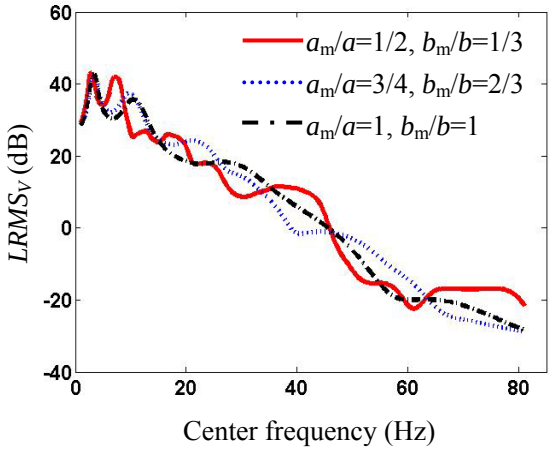

Fig. 13 Logarithmic root-mean-square velocity ($LRMS_v$) spectra of sandwich plate for different lengths (a_m) and widths (b_m) of localized magnetic field (x_{0m}=y_{0m}=0)

4.4 Micro-vibration responses for various magnetic field distributions

The complex modulus of the MRVE core can be changed by the applied magnetic field, and then various magnetic field distributions are considered. The MRVE parameters are as follows: α_0=0.3 MPa, α_1=0.01 MPa·s, β_0=0.3 for applied magnetic field and α_0=0.03 MPa, α_1=0.001 MPa·s, β_0=0.3 for unapplied magnetic field. The influences of the center and region of the localized magnetic field on the root-mean-square velocity response of the MRVE sandwich plate with supported mass at the midpoint are shown in Figs. 13-15. Fig. 13 shows the logarithmic root-mean-square velocity response at the midpoint of the MRVE sandwich plate for different region lengths a_m and widths b_m of the localized magnetic field (x_{0m}=y_{0m}=0). It is obtained that the root-mean-square velocity response changes slightly with the region size covered by the magnetic field under the region larger than certain area, for example, with a_m/a=3/4 and b_m/b=2/3, because the effect of the further increase of the covered region on the damping and stiffness of the first several plate modes becomes slight.

Figs. 14 and 15 show the logarithmic root-mean-square velocity response at the midpoint of the MRVE sandwich plate for different centers (x_{0m}, y_{0m}) of the localized magnetic field (a_m/a=1/4, b_m/b=1/3).

It is obtained that the region center of the localized magnetic field moderately deviating from the plate center (for example, x_{0m}/a=1/6, y_{0m}/b=1/6 with a_m/a=1/4, b_m/b=1/3) can achieve better effectiveness of the root-mean-square velocity response reduction (based on the first two peak responses [39 dB and 26 dB corresponding to that localized magnetic field] in [8, 80] Hz). In consequence, the micro-vibration response of the sandwich plate with supported mass under stochastic support micro-motion excitations can be controlled effectively by using the MRVE core with applied localized magnetic fields.

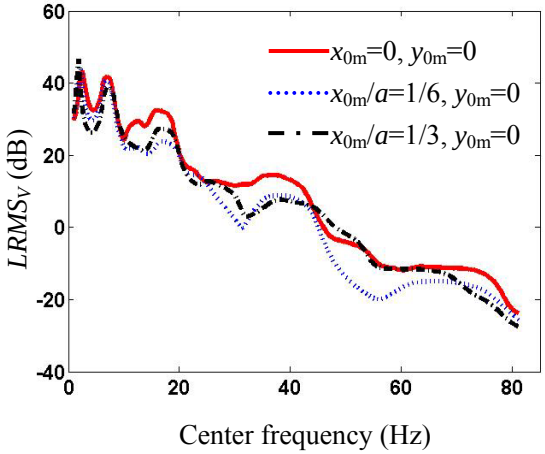

Fig. 14 Logarithmic root-mean-square velocity ($LRMS_v$) spectra of sandwich plate for different centers (x_{0m}, y_{0m}) of localized magnetic field (y_{0m}=0, a_m/a=1/4, b_m/b=1/3)

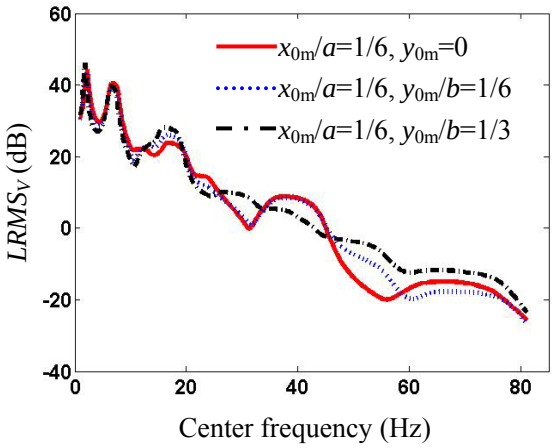

Fig. 15 Logarithmic root-mean-square velocity ($LRMS_v$) spectra of sandwich plate for different centers (x_{0m}, y_{0m}) of localized magnetic field (x_{0m}/a=1/6, a_m/a=1/4, b_m/b=1/3)

5. Conclusions

The stochastic micro-vibration response of a sandwich plate with MRVE core and supported mass under stochastic support motion excitations has been analyzed and calculated to evaluate the micro-vibration suppression capability. The transverse and longitudinal coupled vibration equations for the MRVE sandwich plate with supported mass have been derived from the dynamic equilibrium, constitutive and geometric relations. The simplified ordinary differential equations for the transverse vibration of the MRVE sandwich plate under localized magnetic fields have been obtained. The effects of the supported mass and localized magnetic field on the stochastic micro-vibration response of the MRVE sandwich plate have been taken into account. A frequency-domain solution method for the stochastic micro-vibration response of sandwich plates

with supported mass has been developed by using the Galerkin method and random vibration theory. The frequency-response functions, response power spectral densities and root-mean-square velocity response expressions of the plate in terms of the one-third octave frequency band have been obtained. The developed analysis method is applicable to sandwich plates with supported mass and arbitrary cores described by complex moduli subjected to arbitrary stochastic excitations described by power spectral density functions. Numerical results illustrate that (1) the micro-vibration response of sandwich plates with supported mass under stochastic support motion excitations can be suppressed greatly by using the MRVE core with applied localized magnetic fields; (2) the storage modulus coefficient (α_1) and loss factor (β_0) of MRVE cores have large effects on the micro-vibration response of MRVE sandwich plates with supported mass; (3) the root-mean-square velocity response of the supported mass (m) at the midpoint of the plate is smaller than that in other positions; (4) the thickness (h_2) of MRVE cores larger than a certain value (smaller than 1/3 plate thickness) and the covered region (a_m, b_m) of localized magnetic fields larger than a certain area (smaller than 1/2 plate area) have slight effects on the micro-vibration response of MRVE sandwich plates with supported mass. The above results are valuable for the micro-vibration control design of sandwich plates with supported mass by using MRVE under localized magnetic fields.

Acknowledgments

This work was supported by the National Natural Science Foundation of China under Grant Nos. 11072215, 11432012, 51478429, 51178426, U1234201, and Zhejiang Provincial Natural Science Foundation of China under Grant No. LY15A020001.

References

Amick, H. (1997), "On the generic vibration criteria for advanced technology facilities", *J. Inst. Environ. Sci,*, **40**, 35-44.

Bellan, C. and Bossis, G. (2002), "Field dependence of viscoelastic properties of MR elastomers", *Int. J. Modern Phys. - B*, **16**(17-18), 2447-2453.

Böse, H. (2007), "Viscoelastic properties of silicone-based magnetorheological elastomers", *Int. J. Modern Phys. - B*, **21**(28-29), 4790-4797.

Carlson, J.D. and Jolly, M.R. (2000), "MR fluid, foam and elastomer devices", *Mechatronics*, **10**(4-5), 555-569.

Casciati, F., Rodellar, J. and Yildirim, U. (2012), "Active and semi-active control of structures –theory and application: a review of recent advances", *J. Intel.Mat. Syst. Str.*, **23**, 1181-1195.

Choi, W.J., Xiong, Y.P. and Shenoi, R.A. (2010), "Vibration characteristics of sandwich beam with steel skins and magnetorheological elastomer cores", *Adv. Struct. Eng.*, **13**, 837-847.

Demchuk, S.A. and Kuz'min, V.A. (2002), "Viscoelastic properties of magnetorheological elastomers in the regime of dynamic deformation", *J. Eng. Phys. Thermophysics*, **75**(2), 396-400.

Ditaranto, R.A. (1965), "Theory of the vibratory bending for elastic and viscoelastic layered finite-length beams", *J. Appl. Mech. - ASME*, **32**(4), 881-886.

Dwivedy, S.K., Mahendra, N. and Sahu, K.C. (2009), "Parametric instability regions of a soft and magnetorheological elastomer cored sandwich beam", *J. Sound Vib.*, **325**(4-5), 686-704.

Dyke, S.J., Spencer, B.F., Sain, M.K. and Carlson, J.D. (1996), "Modeling and control of magnetorheological dampers for seismic response reduction", *Smart Mater. Struct.*, **5**(5), 565-575.

Frostig, Y. and Baruch, M. (1994), "Free vibrations of sandwich beams with a transversely flexible core: a high order approach", *J. Sound Vib.*, **176**(2), 195-208.
Ginder, J.M., Clark, S.M., Schlotter, W.F. and Nichols, M.E. (2002), "Magnetostrictive phenomena in magneto-rheological elastomers", *Int. J. Modern Phys. - B*, **16**(17-18), 2412-2418.
Gong, X.L., Zhang, X.Z. and Zhang, P.Q. (2005), "Fabrication and characterization of isotropic magnetorheological elastomers", *Polymer Testing*, **24**(5), 669-676.
Gordon, C.G. (1991), "Generic criteria for vibration-sensitive equipment", *Proceedings of the SPIE*, **1619**, 71-85.
Guan, X.C., Huang, Y.H., Li, H. and Ou, J.P. (2012), "Adaptive MR damper cable control system based on piezoelectric power harvesting", *Smart Struct. Syst.*, **10**(1), 33-46.
Hasheminejad, S.M. and Shabanimotlagh, M. (2010), "Magnetic-field-dependent sound transmission properties of magnetorheological elastomer-based adaptive panels", *Smart Mater. Struct.*, **19**(3), 035006.
Hoang, N., Zhang, N. and Du, H. (2011), "An adaptive tunable vibration absorber using a new magnetorheological elastomer for vehicular powertrain transient vibration reduction", *Smart Mater. Struct.*, **20**(1), 015019.
Hu, W. and Wereley, N.M. (2008), "Hybrid magnetorheological fluid-elastomeric lag dampers for helicopter stability augmentation", *Smart Mater. Struct.*, **17**(4), 045021.
Hwang, J.S., Huang, Y.N., Hung, Y.H. and Huang, J.C. (2004), "Applicability of seismic protective systems to structures with vibration-sensitive equipment", *J. Struct. Eng. - ASCE*, **130**(11), 1676-1684.
Jung, H.J., Eem, S.H., Jang, D.D. and Koo, J.H. (2011), "Seismic performance analysis of a smart base-isolation system considering dynamics of MR elastomers", *J. Intel. Mat. Syst. Str.*, **22**, 1439-1450.
Kallio, M., Lindroos, T., Aalto, S., Järvinen, E., Kärnä, T. and Meinander, T. (2007), "Dynamic compression testing of a tunable spring element consisting of a magnetorheological elastomer", *Smart Mater. Struct.*, **16**(2), 506-514.
Koo, J.H., Khan, F., Jang, D.D. and Jung, H.J. (2010), "Dynamic characterization and modeling of magneto-rheological elastomers under compressive loadings", *Smart Mater. Struct.*, **19**(11), 117002.
Lee, C.L., Su, R.K.L. and Wang, Y.P. (2013), "AGV-induced floor micro-vibration assessment in LCD factories by using a regressional modified Kanai-Tajimi moving force model", *Struct. Eng. Mech.*, **45**(4), 543-658.
Mead, D.J. (1972), "The damping properties of elastically supported sandwich plates", *J. Sound Vib.*, **24**(3), 275-295.
Mead, D.J. and Markus, S. (1969), "The forced vibration of a three-layer, damped sandwich beam with arbitrary boundary conditions", *J. Sound Vib.*, **10**(2), 163-175.
Nakamura, Y., Nakayama, M., Masuda, K., Tanaka, K., Yasuda, M. and Fujita, T. (2000), "Development of active six-degree-of-freedom microvibration control system using giant magnetostrictive actuators", *Smart Mater. Struct.*, **9**(2), 175-185.
Nayak, B., Dwivedy, S.K. and Murthy, K.S.R.K. (2013), "Vibration analysis of a three-layer magnetorheological elastomer embedded sandwich beam with conductive skins using finite element method", *Proc. IME, J. Mech.Eng.Sci.*, **227**(4), 714-729.
Ni, Y.Q., Ying, Z.G. and Chen, Z.H. (2011), "Micro-vibration suppression of equipment supported on a floor incorporating magneto-rheological elastomer core", *J. Sound Vib.*, **330**(18-19), 4369-4383.
Nikitin, L.V. and Samus, A.N. (2005), "Magnetoelastics and their properties", *Int. J. Modern Phys. - B*, **19**(7-9), 1360-1366.
Schoeftner, J. and Buchberger, G. (2013), "Active shape control of a cantilever by resistively interconnected piezoelectric patches", *Smart Struct. Syst.*, **12**(5), 501-521.
Shen, Y., Golnaraghi, M.F. and Heppler, G.R. (2004), "Experimental research and modeling of magnetorheological elastomers", *J. Intel. Mat. Syst. Str.*, **15**(1), 27-35.
Shiga, T., Okada, A. and Kurauchi, T. (1995), "Magnetoviscoelastic behavior of composite gels", *J. Appl. Polymer Sci.*, **58**(4), 787-792.
Spencer, B.F. and Nagarajaiah, S. (2003), "State of the art of structural control", *J. Eng. Mech. - ASCE*, **129**(7), 845-856.

Symans, M.D. and Constantinou, M.C. (1999), "Semi-active control systems for seismic protection of structures: a state-of-the-art review", *Eng. Struct.*, **21**(6), 469-487.
Wang, D.H. and Liao, W.H. (2011), "Magnetorheological fluid dampers: a review of parametric modeling", *Smart Mater. Struct.*, **20**(2), 023001.
Xu, Y.L., Yang, Z.C., Chen, J., Liu, H.J. and Chen, J. (2003), "Microvibration control platform for high technological facilities subject to traffic-induced ground motion", *Eng. Struct.*, **25**(8), 1069-1082.
Yan, M.J. and Dowell, E.H. (1972), "Governing equations for vibrating constrained-layer damping sandwich plates and beams", *J. Appl. Mech. - ASME*, **94**, 1041-1046.
Yang, J.N. and Agrawal, A.K. (2000), "Protective systems for high-technological facilities against microvibration and earthquake", *Struct. Eng. Mech.*, **10**(6), 561-575.
Yeh, J.Y. (2013), "Vibration analysis of sandwich rectangular plates with magnetorheological elastomer damping treatment", *Smart Mater. Struct.*, **22**, 035010.
Ying, Z.G. and Ni, Y.Q. (2009), "Micro-vibration response of a stochastically excited sandwich beam with a magnetorheological elastomer core and mass", *Smart Mater. Struct.*, **18**(9), 095005.
Ying, Z.G., Ni, Y.Q. and Sajjadi, M. (2013), "Nonlinear dynamic characteristics of magneto-rheological visco-elastomers", *Science China, Technological Sciences*, **56**(4), 878-883.
Ying, Z.G., Ni, Y.Q. and Ye, S.Q. (2014), "Stochastic micro-vibration suppression of a sandwich plate using a magneto-rheological visco-elastomer core", *Smart Mater. Struct.*, **23**(2), 025019.
York, D., Wang, X. and Gordaninejad, F. (2007), "A new MR fluid-elastomer vibration isolator", *J. Intel. Mater. Syst. Str.*, **18**, 1221-1225.
Yoshioka, H., Takahashi, Y., Katayama, K., Imazawa, T. and Murai, N. (2001), "An active microvibration isolation system for hi-tech manufacturing facilities", *J. Vib. Acoust.*, **123**(2), 269-275.
Zenz, G., Berger, W., Gerstmayr, J., Nader, M. and Krommer, M. (2013), "Design of piezoelectric transducer arrays for passive and active modal control of thin plates", *Smart Struct. Syst.*, **12**(5), 547-577.
Zhou, G.Y. and Wang, Q. (2005), "Magnetorheological elastomer-based smart sandwich beams with nonconduction skins", *Smart Mater. Struct.*, **14**(5), 1001-1009.
Zhou, G.Y. and Wang, Q. (2006), "Study on the adjustable rigidity of magnetorheological-elastomer-based sandwich beams", *Smart Mater. Struct.*, **15**(1), 59-74.